HiSST: 3rd International Conference on
High-Speed Vehicle Science Technology
14 -19 April 2024, Busan, Korea

Calibration of the MBDA-Subdray Hypersonic Wind Tunnel n°5

A. Duarte Antonio[1], Q. Mouly[1], F. Falempin[1], G. Vilmart[2], C. Brossard[2], P. Nicolas[2]

Abstract

Both intrusive and non-intrusive measuring techniques are employed for calibrating a new hypersonic wind tunnel developed by MBDA France in its Bourges-Subdray test centre under the aegis of DGA (French Ministry of Defence). Flow measurements are made in a 1.5 m diameter test section, at a single hypersonic Mach number. Calibration parameters include static and stagnation pressure, static and stagnation temperature, species concentrations, Mach number and flow direction. Intrusive measurements include Pitot-probes, cone-probes and stagnation temperature probes, gathered in a single cooled rake, specially designed by MBDA France for this tunnel. Some numerical simulation, performed later, predicted a large unstart of the test section due to the big obstruction created by the rake. A radical modification of the rake has been studied (suppression of 3 of the 6 arms) and considered for further test. In the meantime, a test run was performed to validate mechanical and thermal behaviour of the rake as well as its functionalities. Prior to that, a Tunable Diode Laser Absorption Spectroscopy (TDLAS) setup, developed at ONERA, was implemented and tested during an initial test run for non-intrusive *in situ* measurements of water vapour concentration and temperature. Measurement data were successfully obtained and compared with data from RANS simulations performed by MBDA. The comparison exhibits around 10% discrepancy in terms of temperature and water vapour content.

Keywords: *Calibration, Hypersonic-Flow, Probes-Rake, TDLAS, Flow-measurements*

Nomenclature

M –	Mach number
P –	Pressure [Pa]
T –	Temperature [K]
Subscripts	
t –	Stagnation (pressure, temperature…)
s –	Static (pressure, temperature…)

1. Introduction

The MBDA-Subdray Hypersonic Wind Tunnel n°5, developed under the aegis of DGA (French Ministry of Defence) was initially designed to perform free jet tests on hypersonic vehicles. The knowledge of the test environment is fundamental to obtain reliable and accurate vehicles performances. Intrusive rakes are commonly used to collect experimental data across the test section. However, these hypersonic tunnel conditions, like a stagnation temperature T_t greater than 1500 K, involve structural difficulties. The first part of this paper presents the wind tunnel and the test conditions investigated. Then the design of the probe rake is detailed. Some recent numerical simulation showed that the obstruction of the centre part of the rake leads to a large unstarting of the supplying nozzle but also allowed identifying improvements which should lead to a drastically reduced obstruction and should be implemented for further tests. In parallel, a Tunable Diode Laser Absorption Spectroscopy (TDLAS) setup is presented and the results of an initial calibration test without any rake or mock-up, conducted in 2023, are detailed and compared with numerical simulations after their completion.

[1] *MBDA France, alexandra.duarte-antonio@mbda-systems.com*
[2] *DPHY, ONERA, Université Paris Saclay, F-91123 Palaiseau – France, Gautier.Vilmart@onera.fr*

2. Test facility

2.1. Wind tunnel n°5

The new free jet test facility is part of ramjet test centre located in MBDA Bourges-Subdray test centre. It has been designed to allow testing a large scale vehicle in free jet conditions (Fig 1).

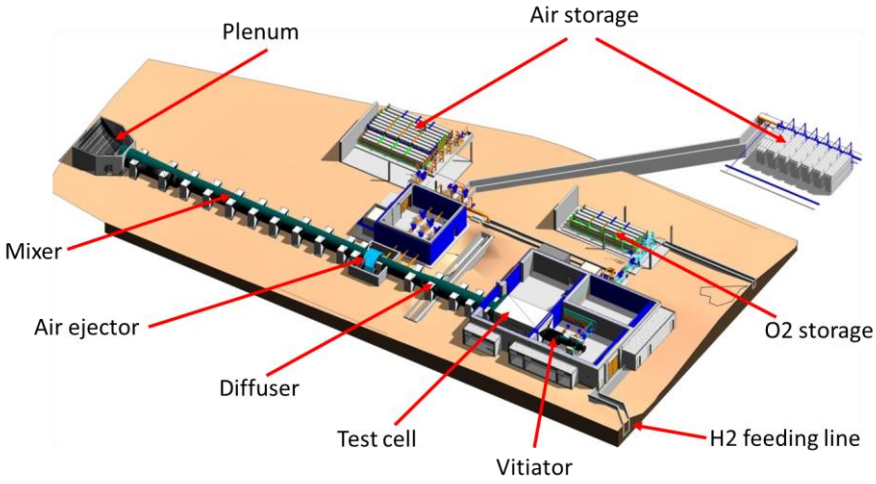

Fig 1 General view of the free jet test facility at MBDA ramjet test centre

A vitiator, burning Hydrogen/Air, provides up to about 70 kg/s of hot gas to feed the supply nozzle with a maximum total temperature of about 2100K (higher total temperature is achievable but not used in operational conditions). The vitiator is equipped with co-axial three-flow injectors - Oxygen/Hydrogen/air – located in a front end and fed by dedicated plenums. The flame tube of the vitiator is cooled by the injected air (Fig 2).

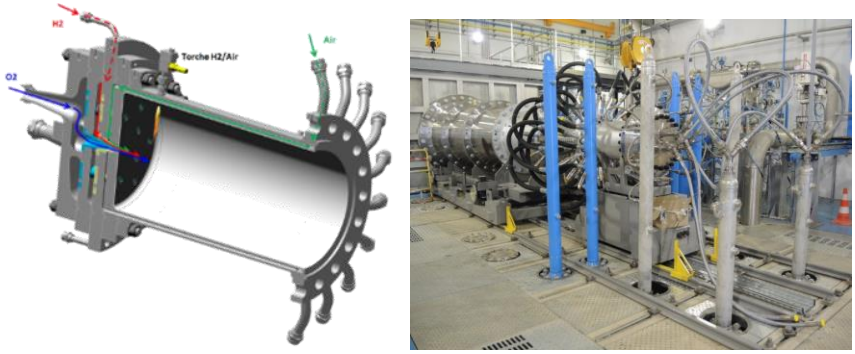

Fig 2 General concept and picture of the vitiator

The supply nozzle has an exit diameter of 1.5m. It is constituted by several sections: an interchangeable water cooled throat giving the Mach number (from Mach 6 to Mach 6+), a first uncooled diverging part protected by zirconia oxide coating, a series of uncooled diverging parts outside the test-cell, a final section embedded in the test-cell with a removable upper part to allow integrating a mock-up partially immerged into the supplying nozzle to take benefit of the complete Mach rhombus (Fig 3).

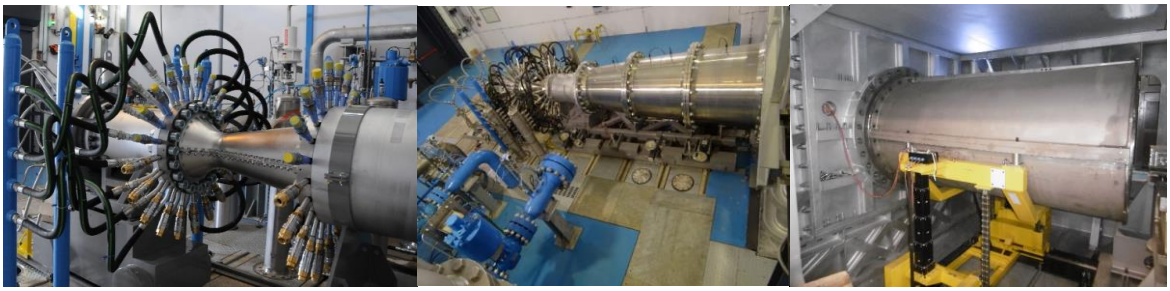

Fig 3 Supplying nozzle

For lower Mach numbers (typically Mach 4.5), a dilution section can be added between vitiator and supplying nozzle to mix hot gas exiting the vitiator with fresh air to get about 120 kg/s of hot gas at needed total temperature.

The test-cell is 4 x 4 X 8 m^3. The test line can be accessed through lateral doors but the mock-up is integrated from the top after test-cell upper wall removal (Fig 4).

Fig 4 Test cell

The diffuser catch is 2 m in diameter. A long diffuser with a slightly converging section is driving the main flow to a circular ejector providing up to 500 kg/s of cold air to suck the main flow. Finally, a mixing section leads to a large plenum which redirects the flow vertically. The total length of the extracting system is about 80m (Fig 5).

Fig 5 Extracting system

2.2. Test Conditions

With the fixed nozzle, a single Mach number M can be obtained in the test section during a run. This paper focuses on the calibration tests performed at a Mach number around 6, with calibration apparatus placed at the test section position. At this Mach number, the usable test period in tunnel is close to 60 s. This duration appears long when designing intrusive devices but it is too short to be able to change calibration methods settings during the run. Furthermore, consecutive tests cannot take place quickly because each test is gas–intensive and requires several days for tanks filling. Therefore, the calibration apparatus was designed to collect as many measurements as possible during a single run.

3. Probe Rake

The initial rake consisted in a 6-pointed-star gathering intrusive probes such as cone-probes, Pitot-probes, and stagnation temperature-probes. This rake was designed to measure test section flow conditions at Mach numbers around 4.5, 6 and 6+. In addition to environment and accuracy measurements constraints, the probe rake met three objectives:

- Maximize the measurements acquired during a single short run
- Maximize the calibration test section area
- Minimize the projected frontal area of the rake.

The following sections describes each probe separately. Then, the initial rake arrangement is presented, as well as rake shape changes suggested according to the numerical simulation results.

3.1. Flow direction

Fig 6 shows one of the 9 stainless steel cone-probes, designed for static pressure and flow direction measurement. Their external shape was built from previous MBDA-probes and parameters extracted

from [1] and [2]. Each probe has 8 static orifices, with a diameter of 1mm. Differential pressure measurement between opposing orifices allows flow path angle determination. According to the highest Mach number simulated in Wind Tunnel n°5, cone half-angle and distance between the cone tip and the static orifices were set. To avoid mutual interference of pitch and yaw, each pair of orifices is accurately located in two perpendicular planes passing through the cone axis. Each static orifice has its own service tubing, connected to one of the miniature pressure scanner placed in the rake, opposite to the probes.

The high total temperature expected led to thermally protect the cone-probes. As cone surface condition is essential for static pressure measurement, the addition of a passive thermal protection was not available, and cone-probes integrate an internal water cooling system, represented in Fig 6. An insert first creates a water jet impact on the cone tip and forms a double skin cooling system with the rest of the cone surface.

After manufacturing, the final dimensions of each cone-probe were precisely measured. Then, their placement on the rake required additional dimensional measurements, to figure the relative position between the probes. These measurements are to be performed before and after each run. In addition to the cone-probes instrumentation, inclinometers are placed in the rake to monitor the star-arms position during a run. According to the numerical mechanical simulations of the star-arms, arms shift is expected only at run startup and shutdown.

Photograph of a cone-probe

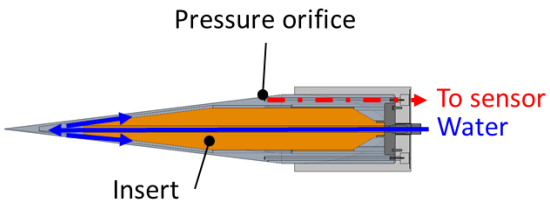

Sectional view of cone-probe model

Fig 6 : Cone-probe design

3.2. Pitot probes

Cooled Pitot-probes, shown in Fig 7, were designed to recover the stagnation pressure. For lower Mach number, stagnation pressure orifice is usually placed in the same probe as the static pressure holes. However, a flat face at the end of the cone-probe in wind tunnel n°5 conditions would affect the static pressure measurements downstream. The Pitot-probes are then separated from the cone-probes. In order to minimize flow blocking, the dimensions of Pitot-probes and their arms were reduced compared to the cone arms, and the rake only holds as many Pitot-probes as cone-probes. Pitot-probes also integrate a water cooling system. A tube walks across the centre of each probe, to connect the stagnation pressure probe orifice to a hole drilled in rake arms and connected to the pressure sensor, opposite to the probe.

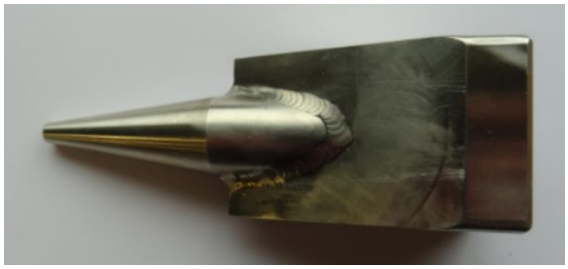

Photograph of a Pitot-probe

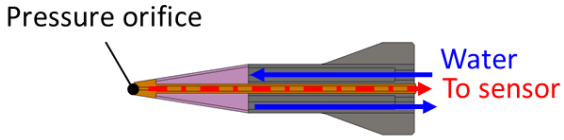

Sectional view of Pitot-probe model

Fig 7 : Pitot-probe design

3.3. Stagnation temperature probes

Vented stagnation temperature-probes were developed based on [3] and [4]. The probe internal hole and two vent holes, spaced 180 degrees apart, are directly drilled in the rake. A removable shield, illustrated in Fig 8, is added to maintain the flow conditions around the sensor, and minimize heat loss. For now, two kinds of thermocouple are designed according to the stagnation temperature expected: thermocouple type B, suited up to 1700 °C, and thermocouple type C, with a longer response time, a shorter lifetime but which can be used up to 2200°C. The number of temperature-probes and the arms shape are similar to Pitot-probes.

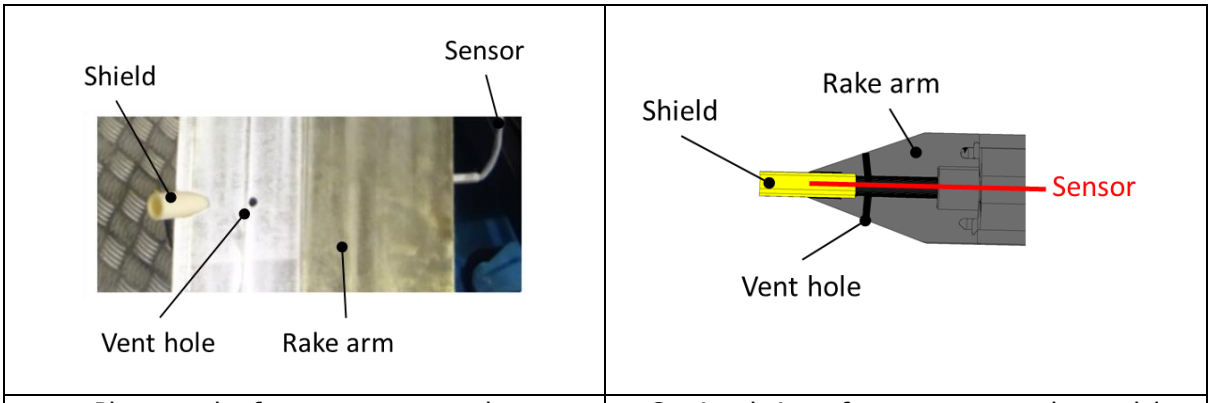

Photograph of a temperature-probe | Sectional view of temperature-probe model

Fig 8 : Stagnation temperature-probe

3.4. Integration into the test line

The probes arrangement on the rake arms was designed to map the greater part of test section. The initial rake integrates only 9 probes of each kind to ensure the measurements are free of rake-related flow interferences or disturbances. Specifically, the space between probes is based on cone-probes and was selected to avoid incident shock impingement from neighbouring cone-probes. The rake configuration is flexible, cone-probes, Pitot-probes, temperature-probes shields and related sensors can be removed and replaced if needed, for example to recover other test conditions.

The rake is mounted on a stand such that, before the run, it can be rotated at 60-degree intervals. Sensors cables follow the stand, protected with a glass fiber braided sleeve and a steel gutter, and are connected to the rake own dedicated data acquisition system (Fig 9).

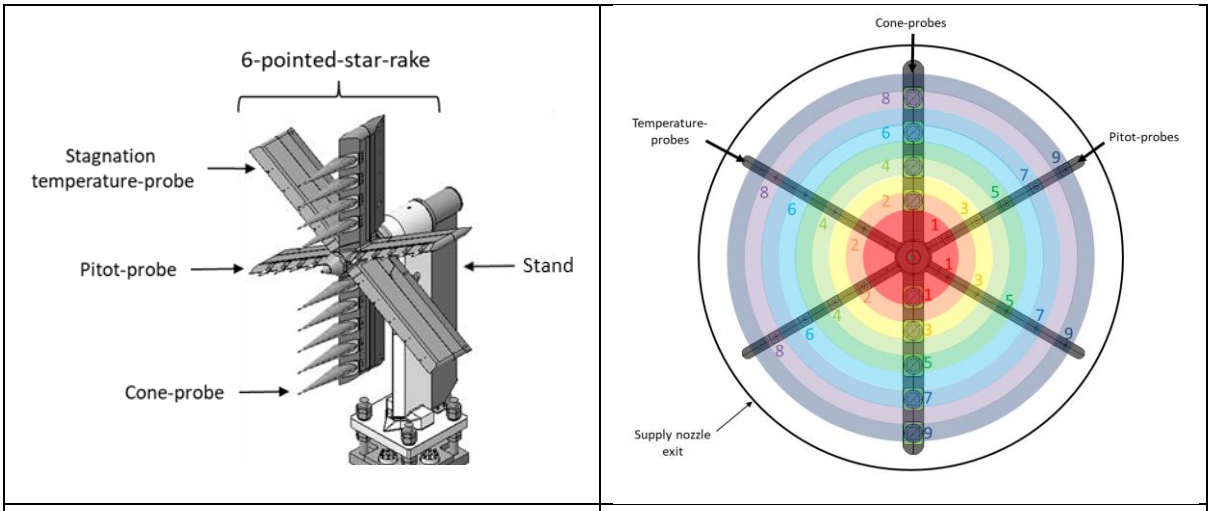

Rake model | Probes distribution

Fig 9 : Initial probe rake

As presented above, one dimensioning criterion for the global rake was its projected frontal area compared to the test section. For the initial rake presented, the selected design maximum area was the one of the flight vehicle, called LEA and presented in [5]. In the same time, as the experience in numerical simulation and the number of wind tunnel n°5 runs increased, simulation methodology, described in [5], has improved. Thanks to this improved methodology, some numerical simulation of the rake in the test section was performed. Results, presented in Fig 10, show that the area occupied by the rake is too big. The rake is completely downstream of the Mach number rhombus, approximately represented by the red colour in Fig 10. Then, a new shape, that corresponds to remove one arm of each kind (cone-probes, Pitot-probes and temperature probes), was studied and evaluated. The results of the same simulation with the new shape are also presented in Fig 10 and reveal a better flow expansion. A rake modification is therefore being considered to perform calibration tests.

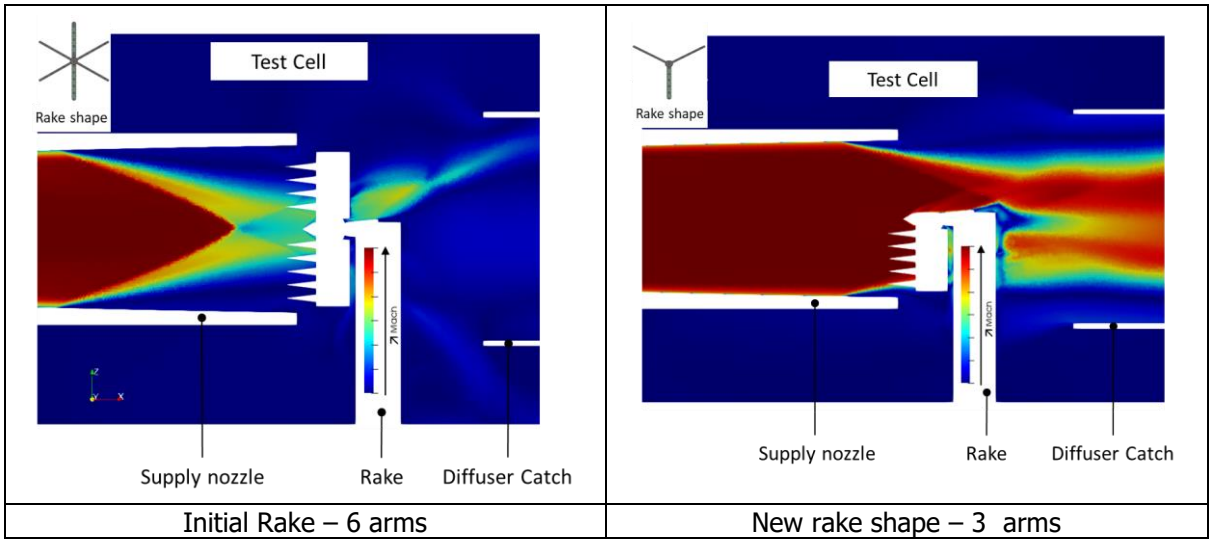

Initial Rake – 6 arms	New rake shape – 3 arms

Fig 10 : Mach field, sectional view in the plane of symmetry

By waiting for this modification to be implemented, the opportunity of one test slot has been taken to test the global mechanical, thermal and functional behaviour of the rake during a test run. As predicted by numerical simulation, the large un-starting of the supplying nozzle led to very harsh mechanical and thermal environment. The rake and its instrumentation survived to these very difficult conditions and all expected measurements were obtained, making the team confident in obtaining valuable data in future tests using the modified rake.

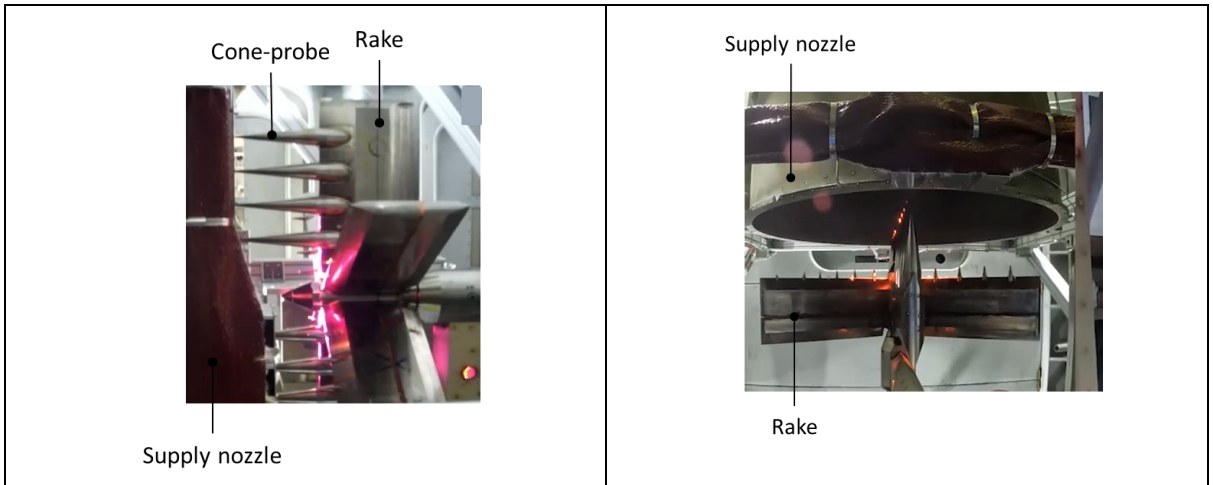

Side view	Bottom view

Fig 11 : Probe rake during harsh environment test run

4. Flow characterization using TDLAS

4.1. Design of the TDLAS instrumentation

The TDLAS non-intrusive optical technique is used for in situ characterization of the flow static temperature and water vapour vitiation downstream of the nozzle exit. This technique has been widely used in combustion studies due to significant advantages, such as high spectral resolution, high chemical selectivity or fast time response (see for instance [6] and [7]). It is compact and can be placed far from the flow; light is transported to the test chamber by using long optical fibers and collimated near the exit nozzle. Selection of a spectrally close pair of transitions, well-adapted to the temperature and water concentration ranges in the probed medium, allows measuring them simultaneously. The major limitation of this technique is that the absorption is line-of-sight integrated, resulting in the absence of spatial resolution along the line.

A TDLAS instrument was designed and fabricated specifically to probe the flow in the wind tunnel N°5. A spectroscopic study was undertaken to select a spectral domain following the procedure described in [8]. In particular, for temperature measurement, the domain must contain two molecular transitions with different sensibilities to it. Indeed, in thermodynamic equilibrium the populations of the molecular states described by the Boltzmann distribution are dependent on the temperature. Consequently, the relative intensity ratio of spectral lines emanating from disparate energy states can serve as a reliable way to determine temperature. The metric used to evaluate this sensibility is the following:

$$S_R(T) = \left|\frac{dR/R}{dT/T}\right| \quad (1)$$

where R is the ratio of the amplitude of the two lines and T is the temperature. It must be at least superior to 1 [8]. Multiple spectra were generated with the Beer-Lambert law using thermodynamic parameters derived from a preliminary simulation of the flow in order to select transitions best suited to probe the flow (P = 15 mbar, T ~ 250 K, X_{H2O} = 0.2). Care was also taken to select transitions with minimal absorption at higher temperature (>500 K) in order to be as insensitive as possible to the absorption in the boundary layer and off-jet regions. For experimental ease, we prioritized the telecom domain to benefit from the recent advances in fibered technology in this domain. After an extensive study with the HITRAN database of the 1.3-1.5 µm domain, we selected the transitions at 7164.075 and 7164.404 cm^{-1}.

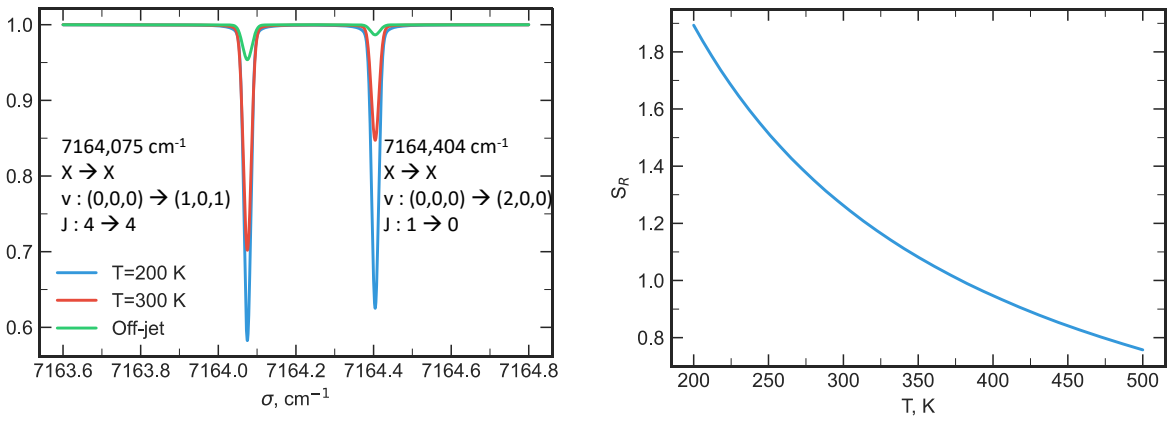

a. b.

Fig. 11 a. Theoretical absorption spectra of H2O calculated with thermodynamic parameters derived from preliminary simulation ; b. Sensitivity of the ratio of the amplitude of the two lines with respect to temperature within the targeted range

As can be seen in Fig. **1**1.a, absorption levels of the two lines are sufficient for the measurement, and evolve differently according to temperature, as is confirmed in Fig. **1**1.b. This figure shows that temperature measurement can be accurate up to about 380 K ; above that value, the sensitivity is inferior to 1, meaning that the ratio of the amplitudes of the two lines stays almost unchanged. In order

to simulate the off-jet absorption, a spectrum calculated for an absorption length of 0.5 m, T = 500 K and the same water vapour molar fraction as in the jet, is added in Fig. **1**1.a. The absorption level is inferior to 5 % for the first line and inferior to 1.5 % for the second line. This ensures that the measurement should be fairly insensitive to off-jet absorption.

Prior to implementation in the wind tunnel, the collimating optics mechanical assemblies were tested on a vibration stand at ONERA. This resulted in multiple adaptations until the absence of misalignment resulting from vibrations could be verified.

4.2. TDLAS set-up

The laser setup used in the experiment is described Fig 12.a. It includes a distributed feedback (DFB) diode laser emitting in the targeted spectral domain. The laser diode injection current is controlled by a National Instruments PXI system. Its emission is divided into two wavelength calibration paths (a reference cell and a Fabry-Perot etalon) and 4 measurement paths. Light is transported to the wind tunnel through long optical fibers, and collimated in a free-space propagating beam by a commercial optical system. After being transmitted through the jet, it is injected in a multimode fiber and detected by a photodetector whose output is digitized by the PXI system with a sampling rate of 10 MS.s^{-1}. Two such laser systems were used simultaneously to generate 8 measurements paths with sufficient energies (around 1-2 mJ). Measurements were obtained at a repetition rate of 10 kHz.

8 absorption lines were installed: 3 horizontal (DG1, DG2, DG3) and 3 vertical lines all crossing the flow in the vicinity of its axis; 1 horizontal line just outside and above the flow, in order to measure the temperature and water concentration in the off-jet region and take it into account when analysing the other lines; and one line crossing the flow horizontally and with an angle, in order to assess the possibility to measure the flow velocity based upon Doppler shifts of the absorption lines (not presented here). Implementation in the wind tunnel is represented in Fig 12.b and 13. Apart from the velocity measurement line, all lines were placed on a square mechanical frame around the test section.

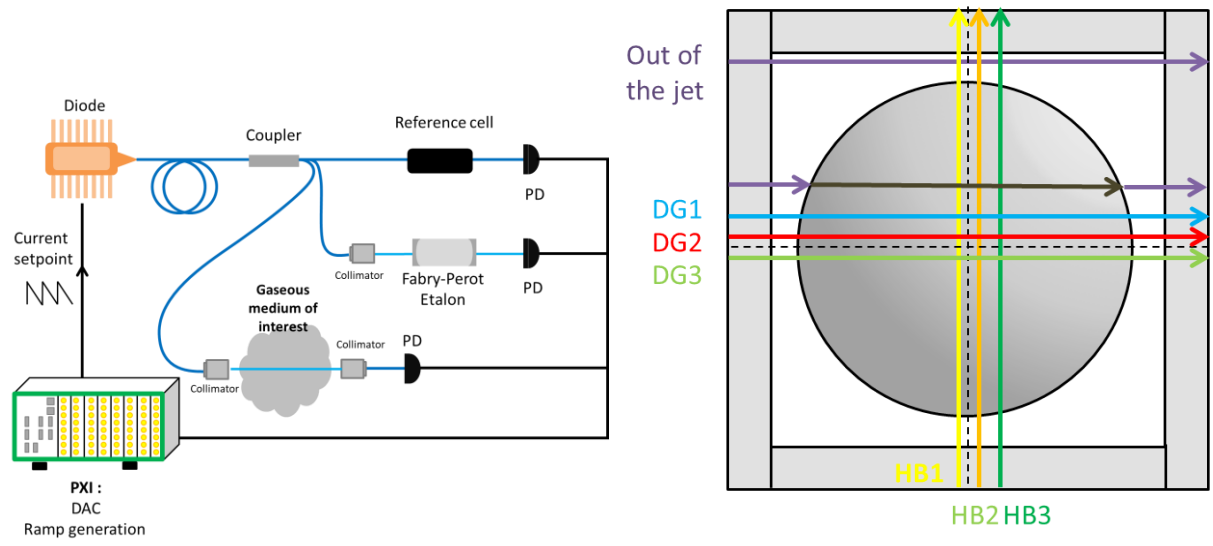

a. b.

Fig 12. a. Scheme of the experimental setup ; b. Implementation in the wind tunnel

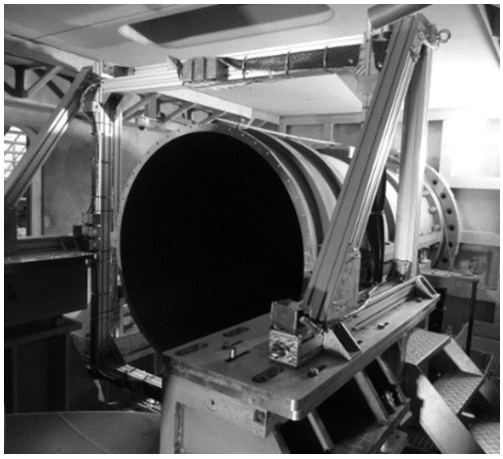

Fig. 13 Photograph of the TDLAS mechanical frame placed around the test section

4.3. Results and Discussion

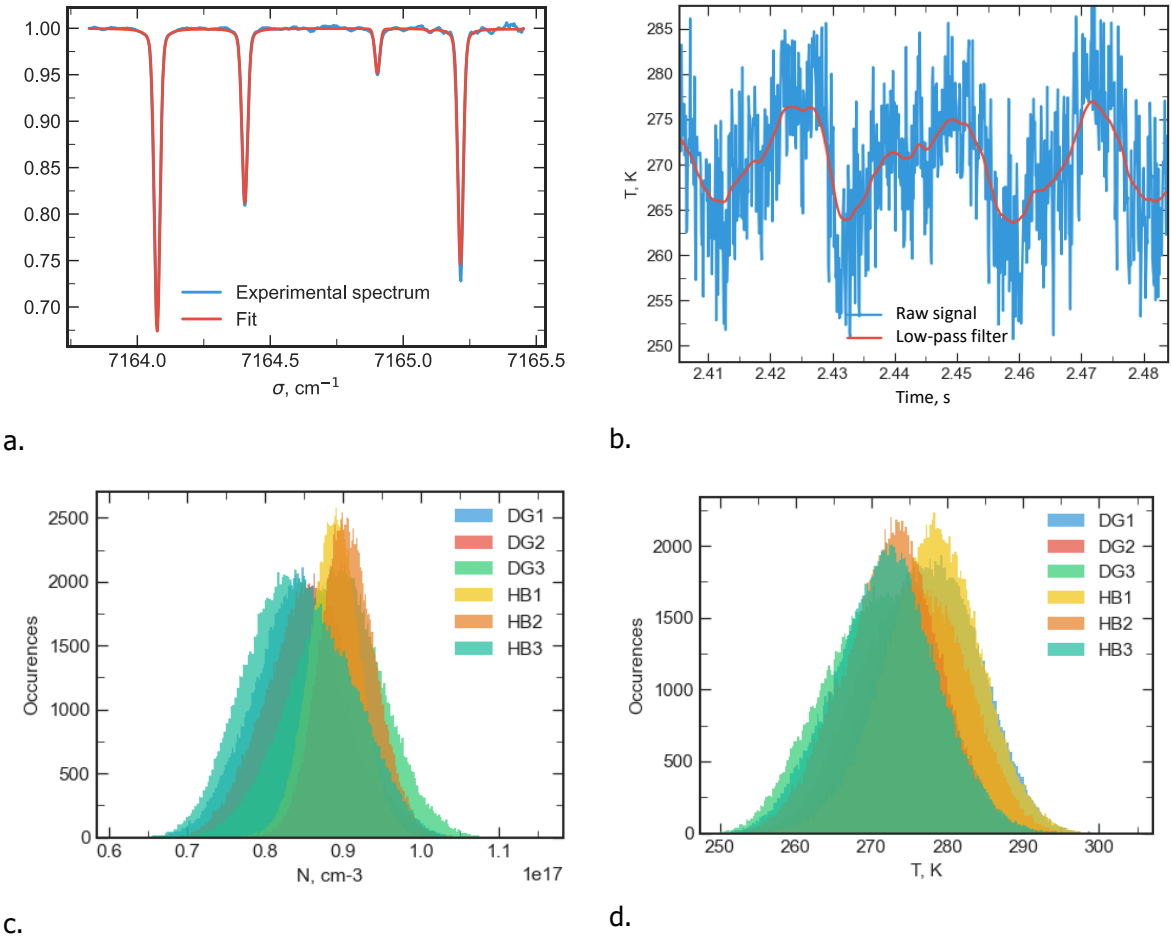

Fig. 14 a. Example of an experimental spectrum and fit ; b. Portion of the time evolution of temperature of the DG2 line showing oscillations, best evidenced after applying a low-pass filter to the signal ; c. Histograms of temperature for the 6 lines ; d. Histograms of water vapour concentration for the 6 lines

The TDLAS setup described in the previous section was tested during a test run without any rake or mock-up inside the test section, leading to a fully started test line.

An example of an instantaneous experimental spectrum is shown in Fig. 14a. It can be observed that the signal to noise is excellent in spite of the harsh experimental environment. In this spectrum, the absorption spectra were corrected from off-jet absorption. In order to do so, the beam positioned above the jet was used to measure the temperature and water vapour concentration of the environment surrounding the jet. Using these values, a new theoretical spectrum was generated to simulate absorption between the position of the collimating optics and the nozzle and used to correct the raw experimental absorption signal. The experimental spectrum in Fig. 14a has also been corrected for a slight distortion induced by the limited bandwidth of custom electronics used to increase the signal level and reduce digitization noise. In a subsequent study, a low-pressure reference cell with approximately the same water vapour concentration was used to reproduce this distortion. This enabled us to characterize the low-pass filter generated by the limited electronics bandwidth and subsequently correct the experimental spectra. Note that the distortion would mainly affect the concentration measurements if not accounted for, because it leaves the ratio of the molecular lines used for temperature measurements mostly unaffected.

The fit in Fig. 14.a obtained with the Beer-Lambert law reproduces very well the experimental spectrum, giving good confidence in the values of the thermodynamic parameters derived from it. The wind tunnel maintains stabilized operation during approximately 12 s. During this period, no temporal drift of the temperature or water vapour concentration was observed. However, small oscillations at 42 Hz are detected, both for temperature and water vapour concentration, for all the lines, as can be seen in Fig. 14.b. The origin of these oscillations has not been investigated so far. It is not clear whether it is really present in the jet or is a side effect of mechanical vibrations of the TDLAS setup. The temperature and water vapour concentration resulting from the fits of the spectra for the 6 lines obtained during the stabilized period are reported in Fig. 14.c and d as histograms. They are quite consistent across all paths, and no overall trend regarding beam positions is observed. On average, static temperature is equal to 275 K, and water vapour concentration to 8.72 10^{16} cm^{-3}, with standard deviations of 6.6 K and 0.5 10^{16} cm^{-3}, respectively.

The experimental results were compared to two RANS simulations: one in which the temperature of the walls of the chamber was fixed at 300 K, and the other assuming wall adiabatic conditions. The results of the simulations are local distributions of the thermodynamic parameters, not directly comparable to the line-of-sight integrated TDLAS measurements. To confront simulations and measurements more directly, the spatially resolved data from simulation were used to generate a synthetic spectrum which was then fitted as for an experimental spectrum, as shown in Fig. 15. This way, simulated integrated values of temperature and concentration were obtained, which could be compared to the experimental data.

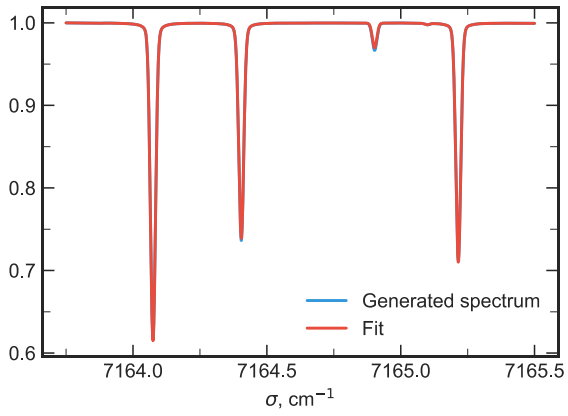

Fig. 15. Spectrum generated from the simulation with limit condition at 300 K and its fit

Results of the comparison can be seen Table 1. In both simulation cases, integrated temperatures are lower by 19-32 K while H_2O concentrations are higher by 1.03-1.19 10^{16} cm^{-3} compared to the mean value of the measurements.

Table 1. Integrated temperature and concentration deduced from simulation

	T (K)	N_{H_2O} (10^{-16} cm^{-3})
Adiabatic	256	9,91
300 K	243	9,75
Mean of measurements	275	8,72

The values deduced from the fits of the experimental spectra could be affected by a few effects, that were evaluated. The first one is possible differences between the actual water vapour and concentration from the nozzle to the collimating optics, and the values used to correct the experimental raw absorption spectra from the off-jet absorption, which are the ones measured with the off-jet line placed above the jet. In order to assess this effect on temperature measurements, the temperature and concentration used to generate spectra representing off-jet absorption and correct experimental spectra were varied from 450 to 1100 K and from 10^{16} to 3.5 10^{16} cm^{-3}, respectively. Subsequently, the newly corrected experimental spectra were fitted once more. Only when using an unrealistically high concentration would the fit lead to a lower temperature as in the simulations. The change of off-jet temperature does not result in a change in the measured in-jet temperature. As predicted when selecting the spectral domain, the off-jet part in the absorption spectra is marginal, and has a limited influence on the values deduced from the fits. A second possible measurement bias could come from evaluating the signal baseline. Because the injection current of the laser diode is modulated to change its wavelength, so is its amplitude. As a result, the absorption spectra are superimposed on a baseline which needs to be evaluated to be removed. It is usually done by fitting the non-absorbing regions of the spectra with a low-order polynomial. This operation can be problematic if the molecular lines are not well separated or if there are few or no non-absorbing regions. This is not the case at all here, as can be seen in Fig. 14.a, meaning that baseline evaluation and removal is not expected to result in any significant bias.

5. Conclusion

When performing free jet testing of a hypersonic air breathing flight system, it is of prime interest to get the most detailed knowledge of the incident flow. In that view, MBDA France and ONERA developed both intrusive and non-intrusive measuring systems to calibrate the different supplying nozzles developed to perform free jet test in the Mach number range 4.5 to 6+. Some preliminary test of the rake, developed by MBDA France, demonstrated the ability of the system to withstand a very harsh mechanical and thermal environment while providing usable data. A design evolution is considered for further tests. The TDLAS setup developed by ONERA was tested during a test run without any rake or mock-up inside the test section, leading to a fully started test line. The system operated well and provided valuable test data. A comparison of acquired results with RANS simulation exhibits around 10% discrepancy in terms of temperature and water vapour content. However, further studies should be performed to better understand how the RANS simulation can be affected by key assumption made and particularly combustion efficiency in the vitiator.

References

1. Mark J. Won : Cone-Probe Rake Design and Calibration for Supersonic Wind Tunnel Models. Ames Research Centre, MS 227-6, Moffett Field, CA 94035-1000 (1999)
2. D. J. Raney, B.Sc.Eng, A.C.G.I, D.I.C. : Flow Direction Measurements in Supersonic Wind Tunnels. C.P. No. 262 (17.502) A.R.C. Technical Report (1954)
3. E. M. Winkler : Stagnation Temperature Probes for Use at High Supersonic Speeds and Elevated Temperatures. NAVORD Rep. 3834, U.S. Navy (1954)

4. P. J. Bontrager : Development Of Thermocouple-Type Total Temperature Probes In The Hypersonic Flow Regime. AEDC-TR-69-25, ARO, Inc, (1969)
5. F. Falempin , A. Duarte, M. Lechevallier, Q. Mouly, J. Lefieux, E. Choquet : Development of a Free Jet test facility aiming at preliminary validating aero-propulsive balance prediction methodology for hypersonic air-breathing vehicles. HiSST-2024-224
6. Webber, M.E, Wang J. Sanders, S.T., Baer D.S., Hanson, R.K.: In situ combustion measurements of CO, CO2, H2O and temperature using diode laser absorption sensors. Proceedings of the Combustion Institute 28, 407-413 (2000)
7. Brown, M.S., Herring, G.C., Cabell, K., Hass, N., Barhorst, T.F., Gruber, M.: Optical Measurements at the Combustor Exit of the HIFiRE 2 Ground Test Engine. AIAA 2012-0857 (2012)
8. Xin Zhou *et al* 2003 *Meas. Sci. Technol.* 14 1459